



Interaction of inorganic and organic compounds of physiological fluids with thermally treated Ti surfaces

Laura Burgos-Asperilla^a, Miriam Gamero^a, M^a. Lorenza Escudero^b,
Concepción Alonso^a, M^a. Cristina García-Alonso^{b,✉}

^aDepartment of Applied Physical Chemistry, Universidad Autónoma de Madrid, 28049 Madrid, Spain

^bDepartment of Materials Engineering, Degradation and Durability, National Centre for Metallurgical Research (CENIM), CSIC, 28040 Madrid, Spain

✉Corresponding author: crisga@cenim.csic.es

Submitted: 18 November 2013; Accepted: 11 May 2014; Available on line: 04 September 2014

ABSTRACT: The study of the interaction between the thermally treated Ti (TT-Ti) at 277 °C for 5 hours and the body fluids, ranging from the simplest to the most complex solution is analysed. Electrochemical techniques such as the measurement of the corrosion potential, electrochemical impedance spectroscopy and the polarization curves have been used. The characterization of TT-Ti has been performed by scanning electron microscopy, atomic force microscopy and X-ray Photoelectron Spectroscopy (XPS). The XPS reveals that the peak intensity associated with phosphate and calcium increases as immersion time does. However, the albumin covers rapidly the surface since the C peak intensity remains constant from the first day to the end of immersion time. The calcium ions have a bridging effect on the electrostatic adsorption of phosphate ions as well as that of albumin and the acidic hydroxyl groups of the oxide layer. The impedance measurement shows that the resistance of the oxide layer immersed in albumin and foetal bovine serum decrease probably due to the formation of organometallic complex. The polarization curves reveal that the presence of proteins decreases the current of anodic branch indicating that the proteins work as a barrier on the surface.

KEYWORDS: Bovine serum albumin; Calcium phosphate; Corrosion; Foetal bovine serum; Titanium; XPS

Citation / Cómo citar este artículo: Burgos-Asperilla, L., Gamero, M., Escudero, M.L., Alonso, C., García-Alonso, M.C. (2014) "Interaction of inorganic and organic compounds of physiological fluids with thermally treated Ti surfaces". *Rev. Metal.* 50(3): e022. doi: <http://dx.doi.org/10.3989/revmetalm.022>.

RESUMEN: *Interacción de compuestos inorgánicos y orgánicos de fluidos fisiológicos con superficies de Ti tratadas térmicamente.* Se estudia la interacción del Ti oxidado a 277 °C durante 5 horas con compuestos orgánicos e inorgánicos presentes en los fluidos fisiológicos, desde la solución más simple a la más compleja. Se han utilizado técnicas electroquímicas como la evolución del potencial de corrosión, espectroscopía de impedancia electroquímica y curvas de polarización, y la espectroscopía de fotoelectrones de rayos X (XPS). El XPS revela que la intensidad de los picos asociados a los iones fosfato y calcio aumenta con el tiempo de inmersión. Sin embargo, la albúmina cubre desde el primer día la superficie, ya que la intensidad de los picos asociados a la presencia de C permanece prácticamente constante hasta el final del ensayo. Los iones calcio actúan como puente de unión entre los iones fosfato y la albúmina, y los grupos hidroxilo ácidos de la capa de óxido. Las medidas de impedancia muestran que la resistencia de la capa de óxido en albúmina y FBS disminuye probablemente debido a la formación de complejos órgano-metálicos. Las curvas de polarización revelan que cuando la solución contiene proteínas, la intensidad de la rama anódica disminuye indicando que las proteínas ejercen un efecto barrera sobre la superficie del Ti.

PALABRAS CLAVE: Albúmina de suero bovino; Corrosión; Fosfato cálcico; Suero bovino fetal; Titanio; XPS

Copyright: © 2014 CSIC. This is an open-access article distributed under the terms of the Creative Commons Attribution-Non Commercial (by-nc) Spain 3.0 License.

1. INTRODUCTION

One of the most important stages in the life of an implant is the initial interaction between biomaterials and the physiological environment of surrounding tissues. Physiological environment is a complex medium composed of inorganic and organic compounds that compete to be adsorbed on the surface of the biomaterial. At the first step, proteins spontaneously adsorb onto the surface together with other inorganic compounds such as phosphates (Healy and Ducheyne, 1992) and calcium (Serro do *et al.*, 1997). However, the sequence of adsorbing species seems to be gradual. Proteins as albumin are the fastest to be adsorbed on metallic substrates, followed by the deposition of the calcium and phosphate ions (Serro *et al.*, 1997). The resulting surface-bound protein layer mediates the subsequent cell attachment through interactions with cell surface receptors (Ratner, 2004). What happens after these first stages will determine the longevity of these biomedical implants. The continuous interaction between the active biological compounds of human body and the biomaterial surface provokes the degradation by corrosion of the materials (Carboneras *et al.*, 2011) within the body leading to the release toxic elements in time. The progressive and continuous ion release may have negative effects on the surrounding and more distant tissues (Lin *et al.*, 2007; Rubio *et al.*, 2008).

The geometrical and chemical properties of biomaterial surfaces direct not only the characteristics of the protein layer but cellular functions such as cell migration, proliferation, modulate phenotypic differentiation and alter the responsiveness to extracellular signals (Kasemo, 2002). The surface state of the biomaterial, i.e. topography, roughness, texture and chemical composition depends strongly on cellular responses (Wójciak-Stothard *et al.*, 1995; Curtis and Varde, 1964). It has recently been revealed that cell adhesion is also influenced by surface features as small as 10 nm (Dalby *et al.*, 2004). These features promote the search of new surface modifications that not only reduce the ion release of Ti surfaces but also simulate the size of the proteins or cell membrane receptors (Kubo *et al.*, 2009; Lord *et al.*, 2010). Many studies have reported that oxidation treatments at different temperatures and oxidation times promote best corrosion and biocompatibility behaviour. Surface modification implemented by oxidation provides nanotopographies that may be relevant in the adsorption of proteins. Escudero *et al.* (2004) and Bello *et al.* (2010) demonstrated that thermal treatment of γ -TiAl at 500 °C and at 800 °C for 1 hour in air can be used to generate highly corrosion-resistant and biocompatible surfaces for implant applications. García-Alonso *et al.* (2003) and Saldaña *et al.*

(2005) established that thermal oxidation treatment of Ti6Al4V at 500 °C or 700 °C for 1 hour improved its *in vitro* biocompatibility. On the other hand, Hwang *et al.* (2003) studied calcium phosphate formation on commercially pure Ti samples that were oxidized from 500 °C to 700 °C for 10 minutes in air. To evaluate the ability of calcium phosphate formation, samples after annealing were soaked in the Eagle's minimum essential medium. They found that well-grained and compact rutile structures could be formed by annealing at 700 °C without CaP formation on the surface. But, an amorphous TiO₂ layer with a heterogeneous structure that was annealed at 650 °C and below had the greatest CaP-forming ability.

Further, the lowest oxidation temperatures can have a beneficial effect on the formation of a high coverage of hydroxylated groups on the surface that act as covalent bonds between organometallic compounds and the oxidized titanium surface, increasing the stability of functional organic overlayers (Jones, 1998). The lowest oxidation temperatures of Ti has a beneficial effect on the formation of a high coverage of hydroxylated groups on the surface that act as covalent bonds between organometallic compounds and the oxidized titanium surface, increasing the stability of functional organic overlayers. Lu *et al.* (2000) determined that the maximum oxidation of Ti surface in an oxygen-rich atmosphere and the maximum OH concentration in a water vapour-rich atmosphere were achieved between 227–327 °C.

In this context, the aim of this work consists of the study of the electrochemical interaction between the Ti surfaces oxidized at low temperature and different inorganic and organic compounds presents in the body fluids, ranging from the simplest to the most complex solution. The influence of each component will be evaluated through the electrochemical response of the oxide layer grown after the oxidation treatment and the chemical composition of the surface by X-ray Photoelectron Spectroscopy (XPS) after several immersion times at the different compounds presents in the body fluids.

2. MATERIALS AND METHODS

2.1. Metallic material

Commercial Ti disks (Goodfellow, France) of 25 mm diameter and 2 mm thickness were used as the test specimens. Their surface was ground in water with SiC abrasive paper of increasing fineness, from 400 to 1200 mesh and finally polished with 9 μ m diamond. The Ti samples were then washed in distilled water and rinsed ultrasonically in ethanol for 10 minutes. The Ti disks were thermally treated at 277 °C for 5 hours (hereafter TT-Ti samples).

2.2. Surface characterization

A scanning electron microscope Jeol-6500F equipped with a Field Emission Gun (FEG) coupled with an Energy Dispersive X-Ray (EDX) spectrometer was used to characterize the surface morphology of the TT-Ti samples after the thermal treatment. The images were taken by using secondary electrons.

An Agilent Atomic Force Microscope (AFM) 5100 equipped with a scanner of maximum ranges of 10 μm in the “x” and “y” directions and 4 μm in the “z” direction was used to obtain roughness data and surface images. The images were acquired by using silicon nitride cantilevers with a nominal probe curvature radius of 10 nm and a force constant of 40 N m^{-1} . Images were acquired at a resolution of 512×512 points. WSxM software of Nanotec was used (Horcas *et al.*, 2007). For morphological imaging of TT-Ti samples tapping-mode AFM microscopy has been used.

The chemical composition at the surface was analyzed using X-ray Photoelectron Spectroscopy (XPS). Photoelectron spectra were obtained with a VG Escalab 200R spectrometer equipped with a hemispherical electron analyzer (pass energy of 50 eV) and a $\text{MgK}\alpha$ ($h\nu = 1254.6$ eV, $1 \text{ eV} = 1.6302 \times 10^{-19}$ J) X-ray source, powered at 120 W. The kinetic energies of photoelectrons were measured using a hemispherical electron analyser working in the constant pass energy mode. The background pressure in the analysis chamber was kept below 2×10^{-8} mbar during data acquisition. The XPS data signals were taken in increments of 0.1 eV with dwell times of 50 ms. Binding energies were calibrated relative to the C1s peak at 284.9 eV. High resolution spectra envelopes were obtained by curve fitting synthetic peak components using the software “XPS peak”. The raw data were used with no preliminary smoothing. Symmetric Gaussian-Lorentzian product functions were used to approximate the line shapes of the fitting components. Atomic ratios were computed from experimental intensity ratios and normalized by atomic sensitivity factors (Wagner *et al.*, 1981).

2.3. Electrochemical cell

The electrochemical cell with a three-electrode setup was used (Alonso *et al.*, 2008). A platinum wire (99.99% purity) served as the auxiliary electrode. All the potentials are quoted with respect to Ag/AgCl reference electrode. The area of the working electrode (TT-Ti disk) exposed to the solution was 0.79 cm^2 for all the experiments. The experiments were performed in solutions thermostated at $25 \text{ }^\circ\text{C} \pm 0.5 \text{ }^\circ\text{C}$.

2.4. Reagents and solutions

All the solutions were prepared with ultrapure water by means of a Millipore Milli-Q system (18.2 $\text{M}\Omega\text{-1}$). Electrochemical tests were performed in different solutions, composed of the same concentration of inorganic and organic compounds as present in Dulbecco’s Modified Eagle’s Medium (DMEM) culture medium from the most simple to the most complex composition (Table 1).

2.5. Electrochemical measurements

The measurement of corrosion potential and Electrochemical Impedance Spectroscopy (EIS) was daily performed during 7 days of testing time. On the last day of testing, quasi-steady-state linear polarization measurements were registered. Before the EIS measurements, the corrosion potential was registered for at least 30 minutes until the potential was stabilized. The EIS experiments were performed at the corrosion potential by applying 10 mV amplitude sinusoidal wave at a frequency range from 10^5 Hz to 10^{-3} Hz spaced logarithmically (five per decade). Gamry equipment was used to perform the electrochemical tests.

The EIS results were analyzed by fitting the experimental impedance data with electrical equivalent circuit models. The equivalent circuit parameters were calculated by fitting the impedance function to the measured spectra by a Non-Linear Least-Squares program (NLLS program) using Z-plot/Z-view for all the frequencies measured. The criteria used in estimating the quality of the fitting were evaluated firstly, with the lower chi-square value and secondly, with the lower estimative errors (in %) for all the components.

Linear sweep voltammetry was used to record the polarization curves at $\pm 0.5\text{V}$ with respect to E_{corr} of TT-Ti electrode after seven days of immersion on each component of the corrosive media (DMEM).

3. RESULTS AND DISCUSSION

3.1. Surface characterization of the TT-Ti

Figure 1 shows the Secondary Electron Image (SEI) micrographs of the Ti surfaces after oxidation at $277 \text{ }^\circ\text{C}$ for 5 hours (TT-Ti). The metallic surface had parallel grooves, typical of the grinding process, demonstrating a homogeneous, roughened oxidized surface on which white spots grew, corresponding with TiO_2 , as verified by EDX (data not shown).

Dimensions of grooves verified by AFM were established between a range of 350 nm and 500 nm in deep and 2–2.5 μm in width. As an example, Figure 2 shows a detailed image from AFM (10 $\mu\text{m} \times 10 \mu\text{m}$)

TABLE 1. Composition of the media (analytical grade reagents)

Solutions	NaCl (mM)	NaH ₂ PO ₄ (mM)	CaCl ₂ (mM)	Glucose (mM)	BSA (g l ⁻¹)
NaH ₂ PO ₄	110	0.91	–	–	–
NaH ₂ PO ₄ + CaCl ₂	110	0.91	1.80	–	–
NaH ₂ PO ₄ + CaCl ₂ + Glucose	110	0.91	1.80	25.00	–
NaH ₂ PO ₄ + CaCl ₂ + BSA	110	0.91	1.80	–	2.52

of the TT-Ti surface showing one groove of approximately 350 nm in deep and 2.5 μ m in width. Considering that filopodia from cells do not to penetrate grooves which are less than 2 μ m in width or 500 nm in depth (Den Braber *et al.*, 1996), the topographical characteristics of the surface seem to be adequate to the dimensions of bone cells. Along the groove and outside, the surface roughness (RMS) varied between 19.43 and 92.40 nm. Surface nanotopography will mainly influence both the orientation of cells on surfaces (Clark *et al.*, 1991) and protein adsorption (Rechendorff *et al.*, 2006).

High-resolution XPS of the Ti2p signal demonstrated that the chemical composition of the oxide film was TiO₂ (Ti2p_{3/2} 458.6 eV in Table 2) in agreement with (Vaquila *et al.*, 1996). Browne and Gregson (1994) suggested that TiO₂ generated at this oxidation treatment corresponded to the anatase form, as they analysed by TEM. This is an important characteristic of the oxide, because not all the Ti oxide structures (rutile, anatase, etc) are equally effective in apatite nucleation. In fact, the anatase phase of titania is highly effective in apatite formation (Uchida *et al.*, 2003).

The high resolution O1s spectrum shows the separation of the O1s band into two components assigned to TiO₂ (529.9 eV) and Ti-OH (531.4 eV in

Table 2). These results are consistent with those of other groups (McCafferty and Wightman, 1999); thus, the presence of the –OH group on the surface is ensured with this oxidation treatment. Hughes-Wassell and Embery (1996) suggested that there are two types of surface hydroxyl groups that coexist on TiO₂ due to the chemisorption of water, which causes the surface to be negatively charged at physiological pH. In our case, hydroxyl groups are present on the TT-Ti surface, which should enhance the formation of CaP on the surface as literature supports (Hwang *et al.*, 2003).

The high resolution C1s spectrum shows only one peak at 284.8 eV representing carbons in a hydrocarbon environment (C-C, C-H) (Wagner *et al.*, 1992).

3.2. Characterization of TT-Ti surfaces after immersion in the different components of culture medium

Table 2 shows the assignation of characteristic peaks of the high-resolution XPS of the TT-Ti surfaces after immersion for 7 days in P, PCa, PCaG, BSA and FBS media. This information will be very useful to further simulate the equivalent circuit model of the interface created between the TT-Ti and each different solution that can help to the interpretation of the electrochemical results.

The XPS spectrum of TT-Ti immersed in the P solution is similar to that obtained for TT-Ti surface in air. Ti2p signal appears with a similar intensity, but lower atomic percentage (Table 2). However, the intensity of Ti-OH band at 531.4 eV has increased with respect to the original oxidized surface possibly due to the chemisorption of OH-group from water molecules. A band that corresponds with PO₄³⁻ at 133.3 eV has appeared in a lower atomic intensity, 1.5 at%. The high resolution O1s spectrum shows the separation of O1s band in two components assigned to Ti-O-Ti and Ti-OH (Fig. 3), because the presence of P is too small to be assigned to the P=O- bond (531.3 eV) (Table 2). The high resolution C1s spectrum can be resolved in three peaks: one at 284.8 eV representing carbons in a hydrocarbon environment (C-C, C-H) and the others at 286.3 and 288.4 eV representing carbons in C=O and O-C=O bond (Mantel and Wightman, 1994).

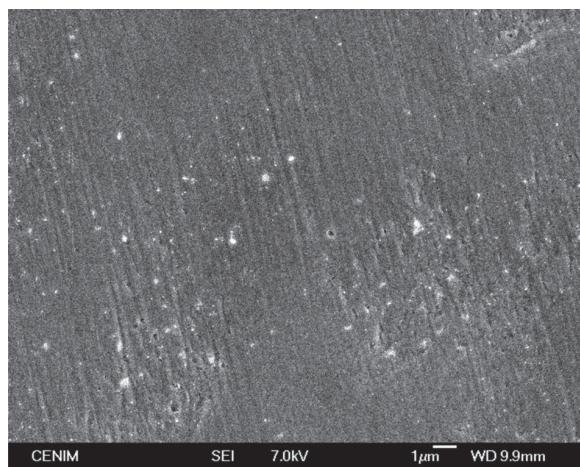


FIGURE 1. SEM image of Ti sample thermally treated (TT-Ti) at 277 °C during 5 hours.

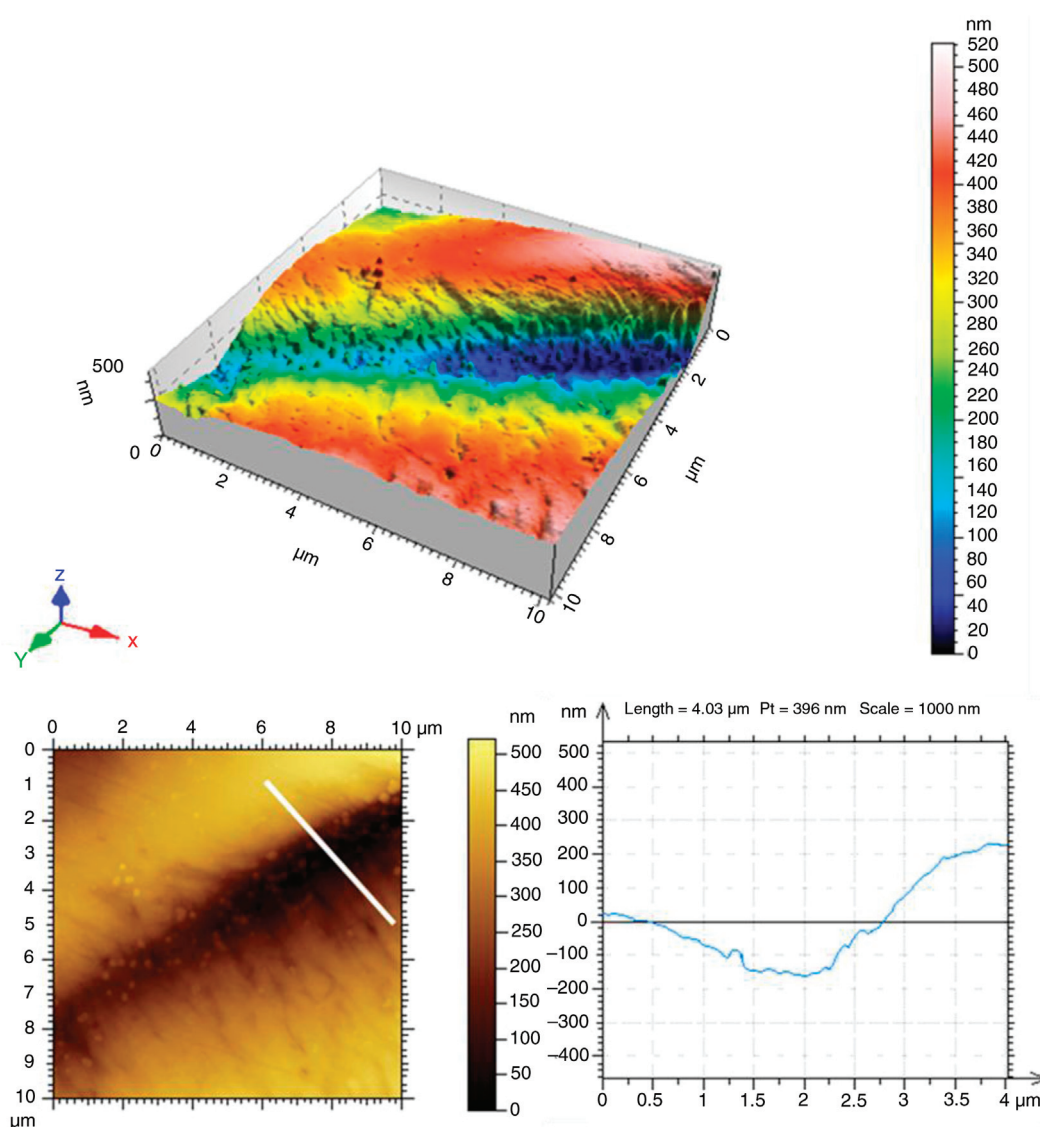


FIGURE 2. Tapping mode AFM image of TT-Ti sample with height profile.

After immersion in the PCa solution, the Ti2p spectrum shows the characteristic peak of Ti-O-Ti with similar intensity (Table 2), but atomic percentage continues decreasing, due to the incorporation of Ca in the surface. The band for Ca2p3/2 appears at 347.9 eV corresponding to CaHPO₄. The presence of calcium ions favours the phosphate ions attraction towards the negatively charged Ti surface. The C1s, O1s and P2p spectra are similar to that in absence of calcium. The Ca/P ratio after the deposition process for seven days (1.3/1.4 = 0.9), is lower than the standard value (1.67) for apatite formation.

The general spectrum when samples are immersed in the PCaG solution changes drastically. The high resolution C1s spectrum shows a broadening with

a contribution of three different components corresponding to carbon in different environments: the first peak, at the lowest binding energy, is assigned to carbon bonded to C or H (C-C, C-H groups); the second peak is attributed to carbon in C=O bond and the third peak, at the highest binding energy, includes the signal for carbon in O-C=O (Mantel and Wightman, 1994) (Fig. 3; Table 2). The shape of the O1s spectra has also changed (Fig. 3). The intensity of the main component corresponding to Ti-O-Ti band has decreased (Table 2) indicating the increment of the surface coverage for the adsorbed glucose. Due to the presence, the adsorbed quantity of glucose on the surface is so large that the underlying titanium surface is masked and the intensity

TABLE 2. XPS binding energies for different peak components of TT-Ti, P/TT-Ti, PCa/Ti-TT, PCaG/Ti-TT, BSA/Ti-TT and FBS/Ti-TT samples

Surface	Element	Atomic (%)	Assignment	Energy /eV	Intensity (a.u.)			
TT-Ti	C1s	3.5	C-C, C-H	284.8	4366			
	O1s	73.0	TiO ₂	529.9	20762			
	Ti2p	23.5	Ti-OH	531.4	4598			
TT-Ti/P	C1s	36.9	TiO ₂	458.6	16510			
			C-C, C-H	284.8	4438			
			C=O	286.3	1172			
	O1s	42.7	O-C=O	288.4	760			
			TiO ₂	529.9	21600			
			Ti-OH	531.4	7874			
TT-Ti/PCa	Ti2p	18.9	TiO ₂	458.5	17613			
			P2p	1.5	PO ₄ ³⁻	133.3	342	
			C1s	26.7	C-C, C-H	284.8	3490	
	TT-Ti/PCaG	C1s	26.7	C=O	286.5	1095		
				O-C=O	288.5	666		
				O1s	53.8	TiO ₂	529.9	21200
TT-Ti/PCaG		Ti2p	16.8	Ti-OH	531.4	6863		
				TiO ₂	458.6	17305		
				P2p	1.3	PO ₄ ³⁻	133.5	316
	TT-Ti/PCaG	Ca2p	1.4	CaHPO ₄	347.9	1092		
				C1s	60.4	C-C, C-H	284.8	4902
				C=O	286.3	3771		
TT-Ti/BSA		O1s	30.7	O-C=O	288.2	2155		
				TiO ₂	530.1	8894		
				O=C-O	531.8	5820		
	Ti2p			7.5	TiO ₂	458.6	7955	
	P2p			0.8	PO ₄ ³⁻	133.5	189	
	Ca2p			0.6	Ca ²⁺	347.1	375	
	TT-Ti/BSA	C1s	63.3	C-C, C-H	284.8	5797		
				C-NH-, C-O	286.3	3810		
				CO-NH-, COOH	288.1	2856		
		O1s	13.7	TiO ₂	529.9	5247		
				C=O, CO-NH-, COOH	531.6	8806		
				Ti2p	5.2	TiO ₂	458.6	4750
TT-Ti/FBS	N1s	17.8	-O=C-NH-, -NH ₂	400.4	4711			
			C1s	57.7	C-C, C-H	284.8	5085	
					C-NH-, C-O	286.4	3347	
	CO-NH-, COOH	288.1			2409			
	O1s	23.8			TiO ₂	530.1	4281	
					C=O	531.9	7984	
					Ti2p	3.4	TiO ₂	458.6
	P2p	0.3	PO ₄ ³⁻	133.6	70			
			Ca2p	0.2	Ca ²⁺	347.7	144	
					N1s	14.6	-O=C-NH-, -NH ₂	400.8

and atomic percentage of Ti2p peak is very low (Table 2). In this case, the presence of phosphate and calcium is not significant indicating that the glucose

adsorption on the titanium surface either prevents the formation of CaHPO₄ or the adsorption layer is thick enough to make it impossible to detect it.

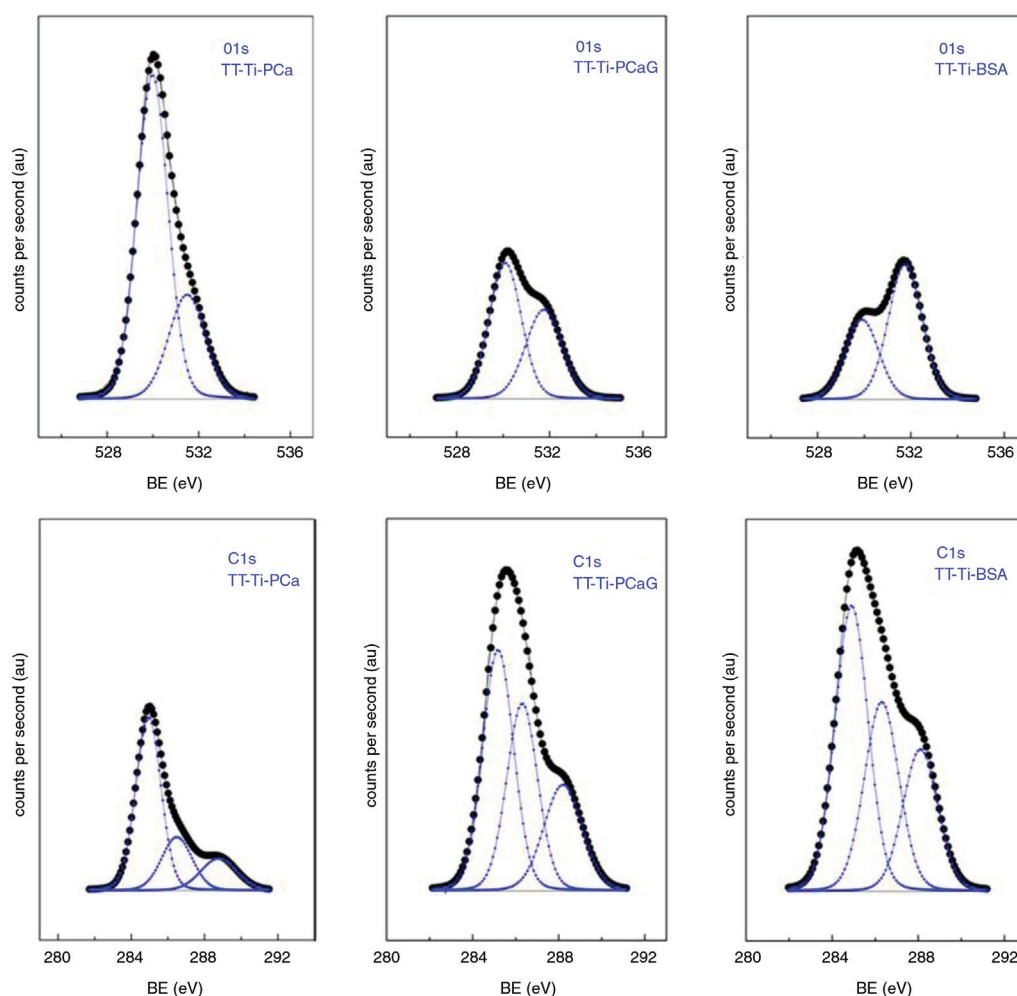


FIGURE 3. High-resolution XPS of O1s and C1s for PCa, PCaG, and BSA after 7 days of immersion.

The spectrum measured after seven days in BSA solution is similar to that obtained for Ti in glucose solution. After the deconvolution of the C1s spectrum three peaks are obtained: (1) 284.7 eV for C-C, C=C and C-H bonds; (2) 286.3 eV being C=O bond; (3) 288.1 eV includes signals from peptide bond (CO-NH-) and acidic groups (COOH). These well-identified bonds correspond to the different chemical groups present in the albumin molecule. Both C1s signal and N1s band come from adsorbed protein. The N1s peak is symmetric, centred at 400.4 eV, corresponding to $-\text{NH}_3^+$. In fact, the strong adsorption of albumin was most likely due to protonated and positively charged amino groups (e.g., histidine, lysine, and arginine). TT-Ti has a negative charge, and positively charged amino groups in albumin act as anchoring sites in the region of contact between the protein and titanium surface. In accordance with these results the O1s band shows two components: 529.9 eV (Ti-O-Ti) and 531.6 eV (O=C-OH, -O=C-NH) (Fig. 3). The Ti-O-Ti band hardly appears (Table 2) due to the

BSA protein adsorption. The absence of phosphate as well as calcium on the TT-Ti surface is noteworthy. Previous studies (Serro do *et al.*, 1997; Lima *et al.*, 2001; Muñoz and Mischler, 2007) indicate that there is a competition between albumin adsorption and phosphates, since phosphate ions may compete with the carboxyl groups of the albumin for exchanging with the basic hydroxyl groups. Calcium is also known to increase the albumin adsorption probably due to calcium bridging between albumin and Ti surface (Clark *et al.*, 1991; Kubo *et al.*, 2009).

No significant differences with respect to the albumin spectra were obtained for TT-Ti surfaces immersed in FBS after seven days (Table 2). This is probably due to the fast adsorption of BSA on the surface that impedes the incorporation of other components such as Ca and P. Nevertheless, small P and Ca amounts have been detected on the TT-Ti surfaces.

The heterogeneity of the roughness in TT-Ti surfaces can promote that other species, such as Ca and P, can be also adsorbed on specific sites where

adsorption of organic molecules is not so facilitated. On the other hand, the oxidation treatment provides a higher amount of OH-group on the surfaces that can be used to promote the adsorption not only of the organic molecules but also inorganic species.

4. ELECTROCHEMICAL RESULTS

4.1. Evolution of open circuit potential, E_{corr}

Figure 4 shows the evolution of the corrosion potential of TT-Ti samples immersed in the different solutions over time, from 0 to 7 days. Two different trends can be observed in the evolution of E_{corr} of TT-Ti surfaces immersed in the different media throughout the testing time. The evolution of the corrosion potential of TT-Ti surfaces immersed in P, PCa and PCaG is rising towards anodic potentials. However, TT-Ti surfaces immersed in BSA and FBS (Fig. 4) show E_{corr} constant over the 7 days, maintaining near -0.080 V. The incorporation of P and Ca in the surface promotes less active surface that agree with the results obtained in other works (Mareci *et al.*, 2009). However, albumin is quickly adsorbed on the surface achieving a stationary state from the first day of testing at more active potentials.

4.2. Evolution of Electrochemical Impedance Spectroscopy (EIS)

The evolution of the impedance modulus and shift-phase angle versus frequency Bode diagrams of the TT-Ti samples after seven days of immersion in the PCa, BSA and FBS media appear in Figure 5.

The impedance measurements in the P and PCa media show the same behaviour so only the results from the PCa medium are shown (Fig. 5a).

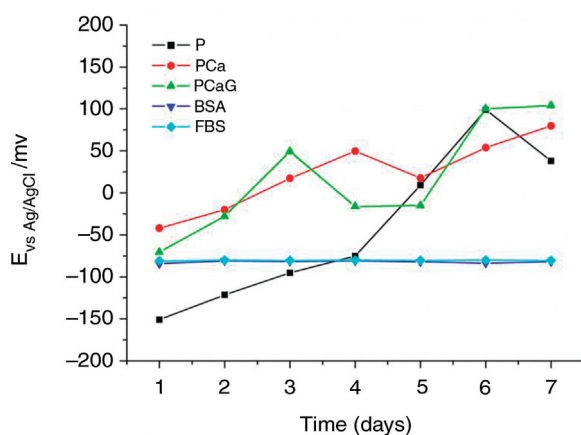


FIGURE 4. OCP vs Time of P/TT-Ti (■), PCa/TT-Ti (●), PCaG/Ti-TT (▲), BSA/Ti-TT (▼) and FBS/Ti-TT (◆) during 7 days.

It can be observed at the high frequencies a plateau in the impedance modulus Bode diagram corresponding to the electrolyte resistance of each solution. At decreasing frequencies (from 100 to 0.01 Hz) the slope of about -0.9 can be attributed to one capacitor in parallel with a resistance formed on the TT-Ti in contact with each solution. At the lowest frequencies, the phase angle is increasing from -60° (first day) to near -90° (seventh day) i.e. the system evolves towards a capacitive response.

In general, the EIS results for TT-Ti immersed in inorganic media reveal capacitive behaviour due to the control exerted by the formation of TiO_2 generated with the oxidation treatment.

The impedance plots of TT-Ti surfaces immersed in BSA and FBS solution for 1 and 7 days (Fig. 5b and c) indicate that the electrochemical response is constant from the first to the last day of testing. At low frequencies (10^{-2} and 10^{-3} Hz), the slope of the impedance modulus changes corresponding with a decrease in theta (-90° to -20°) due to the definition of the oxidized surface resistance. Comparing with the P and PCa media, impedance plots show a more active system because angle does not evolve to higher values (-90 in the other cases) and impedance values at the lowest frequencies has a trend to an horizontal line. in case c). These results agree with the thermodynamic trends observed through the corrosion potential.

The impedance diagrams have been fitted considering the electrical equivalent circuits of Figure 6. The next electronic elements that have been chosen in the circuit were: R_s , the electrolyte resistance measured between the working and reference electrodes, R_2 and CPE2 are the resistance and the pseudo capacitance both corresponding to the outer interface (depending on each component of the solution), associated with the competitive adsorption of molecules onto TT-Ti surfaces; and R_1 and CPE1 are the resistance and the Constant Phase Element, simulating a non-ideal behavior of the capacitor, associated with the oxidized surface and. The impedance of CPE is $Z = 1/[T(j\omega)^n]$ and is generally used when there is a distribution of the relaxation times as a result of non-homogeneous surfaces. The results obtained by the fitting for TT-Ti immersed for 7 days in each solution is given in Figure 7 and Table 3.

The results obtained from the impedance spectra measured for TT-Ti immersed in NaH_2PO_4 and ($\text{NaH}_2\text{PO}_4 + \text{CaCl}_2$) can be assigned to the circuit shown in Figure 6a. The best fitting to the experimental data is given by an equivalent circuit characterized by a unique time constant due to the electrochemical response of the oxide film on the TT-Ti surfaces. In general, the CPE1 and R_1 are practically constant over exposure time (Fig. 7). CPE1 is associated with the interface formed between the Ti-OH of the oxide layer on TT-Ti

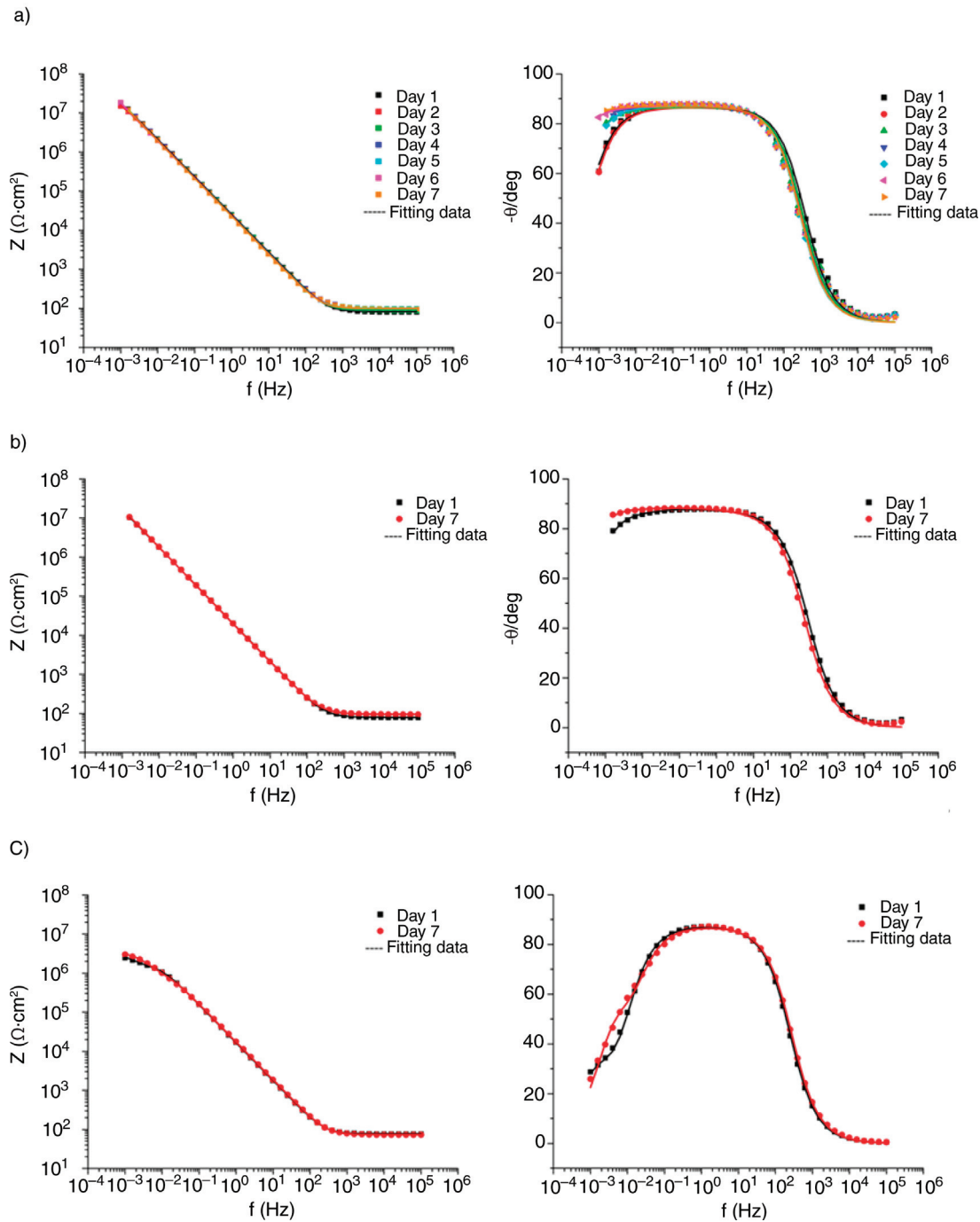


FIGURE 5. Impedance modulus and phase angle diagrams versus frequency of the Bode plots for: a) PCa/TT-Ti, b) BSA/Ti-TT and c) FBS/TT-Ti, during 7 days. — Fitting data.

and the solution, in which some Ti-OH bonds have been replaced by Ti-OP groups, as could be verified by XPS (Table 2). It is known that the H_2PO_4^- and HPO_4^{2-} can form a strong complexing bond with Ti by an exchange reaction with the basic hydroxyl groups (Healy and Ducheyne, 1992; Ouerd *et al.*, 2007).

When the calcium is added to the phosphate solution, R1 is practically constant over exposure time and CPE1 slightly increase with the exposure time, especially from the first to the fourth day of immersion (Fig. 7). Nevertheless, CPE1 is lower and R1 is slightly higher than those values obtained in P solution. This slight increase in CPE1 and R1 correspond

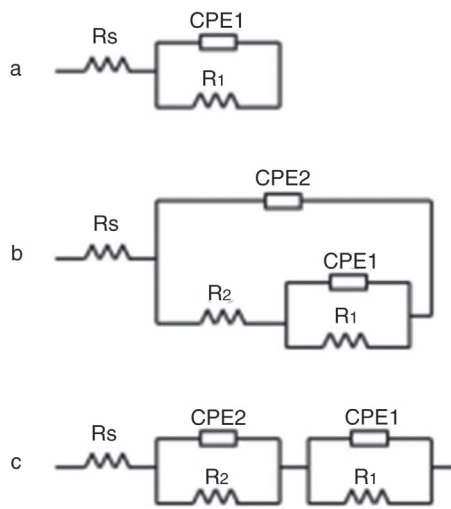


FIGURE 6. Equivalent electrical circuits used for fitting.

to the incorporation of both calcium and phosphate ions through the acidic hydroxyl groups (Ti-OH_2^+) (Ellingsen, 1991; Healy and Ducheyne, 1992) of TT-Ti surfaces or the formation of CaHPO_4 , identified by XPS through the band at 347.9 eV (Table 2). The incorporation of phosphate and calcium ions into the oxide film on titanium has been found both in vivo (Sundgren *et al.*, 1986) and in vitro (Hanawa and Ota, 1991). According to Lima *et al.*, 2001 (Serrado *et al.*, 1997) calcium phosphate films are slowly formed in a period of between 1 and 2 weeks. The rate of in vitro precipitation of an HA- or HCA-like layer on titanium was found to be several orders of magnitude slower than, for example, on bioactive ceramics (Ducheyne and Healy, 1991; Burgos-Asperilla *et al.*, 2010). Furthermore, osseointegration of titanium implants usually takes several months (Albrektsson *et al.*, 1994) which gives us some idea about the slow growth kinetics.

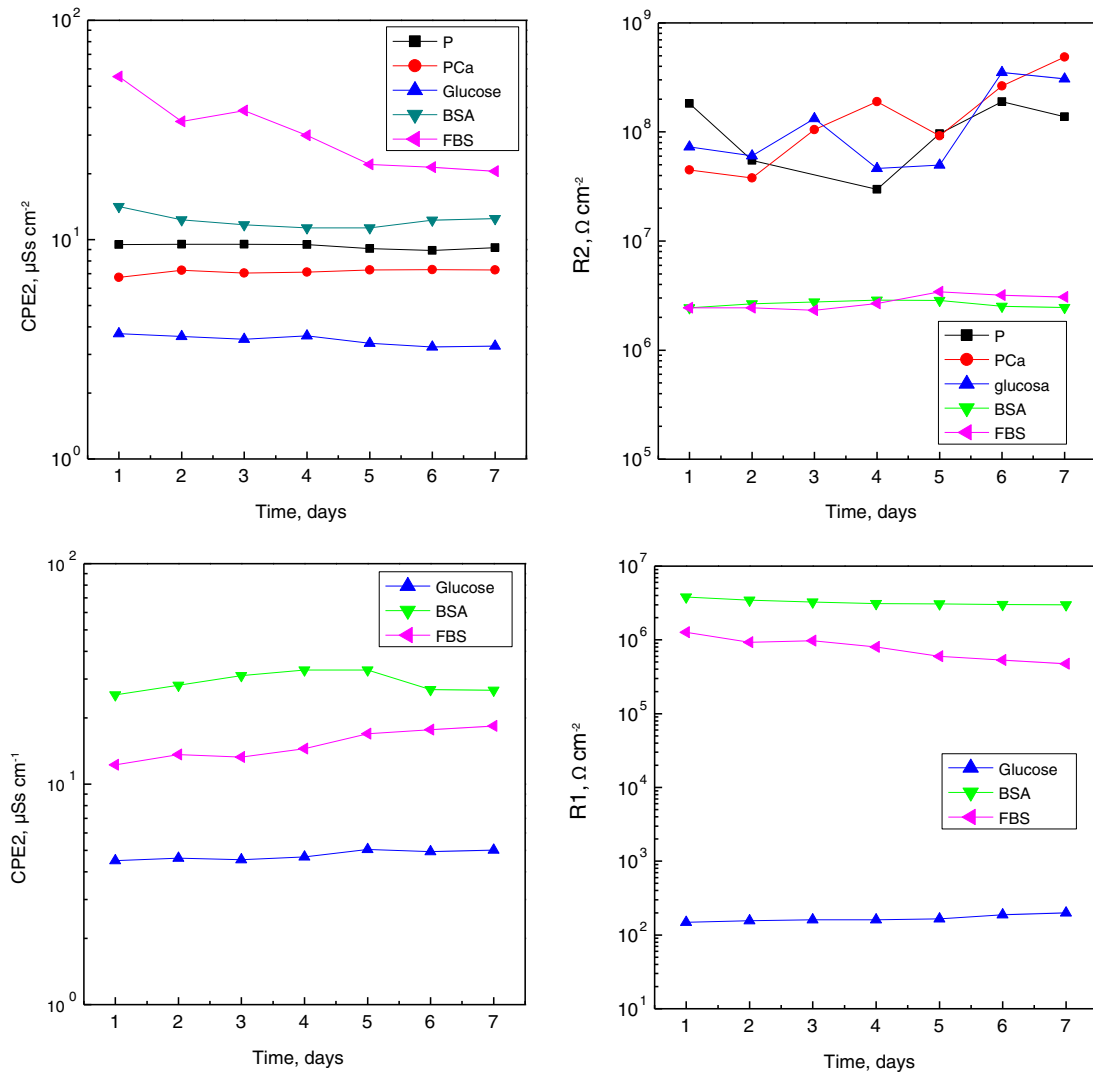


FIGURE 7. Evolution of electric components of the equivalent circuit versus immersion time.

TABLE 3. Experimental data from the impedance diagrams and fitting results, obtained from the simulation by using equivalent circuits of Figure 7, P/TT-Ti, PCa/Ti-TT, PCaG/Ti-TT, BSA/Ti-TT and FBS/Ti-TT at several testing times

Media	Time (days)	C _{exp} (398Hz) (μF cm ⁻²)	Re (Ω)	Z _{threshold} (Ω cm ²)	Rs (Ω)	R2 (Ω cm ²)	CPE2 (μSs cm ⁻²)	n2	R1 (Ω cm ²)	CPE1 (μSs cm ⁻²)	n1	χ ²
P	1	5.96	137.3	1.33·10 ⁷	141.9	–	–	–	1.82·10 ⁸	9.48	0.954	9.26·10 ⁻³
	2	5.99	136.5	1.24·10 ⁷	140.7	–	–	–	5.48·10 ⁷	9.53	0.954	8.69·10 ⁻³
	4	6.06	135.8	1.16·10 ⁷	140.3	–	–	–	2.97·10 ⁷	9.49	0.957	8.88·10 ⁻³
	5	5.98	135.0	9.23·10 ⁶	139.8	–	–	–	9.64·10 ⁷	9.11	0.963	1.28·10 ⁻²
	6	5.92	136.0	1.48·10 ⁷	140.6	–	–	–	1.89·10 ⁸	8.92	0.965	1.41·10 ⁻²
	7	6.01	136.2	5.93·10 ⁶	141.4	–	–	–	1.38·10 ⁸	9.20	0.963	1.47·10 ⁻²
	PCa	1	4.59	100.7	1.77·10 ⁷	104.4	–	–	–	4.49·10 ⁷	6.72	0.963
2		4.81	117.9	1.51·10 ⁷	122.7	–	–	–	3.78·10 ⁷	7.24	0.962	1.48·10 ⁻²
3		4.79	111.3	1.17·10 ⁷	115.9	–	–	–	1.05·10 ⁸	7.04	0.963	1.50·10 ⁻²
4		4.76	122.2	7.95·10 ⁶	127.9	–	–	–	1.89·10 ⁸	7.10	0.965	2.03·10 ⁻²
5		5.16	123.6	1.15·10 ⁷	128.2	–	–	–	9.21·10 ⁷	7.28	0.967	1.14·10 ⁻²
6		4.95	119.4	1.83·10 ⁷	124.6	–	–	–	2.64·10 ⁸	7.29	0.966	1.82·10 ⁻²
7		4.91	120.4	1.19·10 ⁷	125.8	–	–	–	4.87·10 ⁸	7.27	0.966	2.07·10 ⁻²
PCaG	1	6.17	98.5	1.03·10 ⁷	99.2	148.60	4.50	1.000	7.32·10 ⁷	3.73	0.930	1.12·10 ⁻³
	2	6.08	104.8	1.03·10 ⁷	105.4	155.79	4.61	1.000	6.05·10 ⁷	3.62	0.935	1.51·10 ⁻³
	3	5.99	106.3	1.07·10 ⁷	106.9	161.08	4.54	1.000	1.33·10 ⁸	3.52	0.938	1.88·10 ⁻³
	4	6.15	104.2	1.01·10 ⁷	105.0	160.45	4.68	1.000	4.63·10 ⁷	3.64	0.936	1.90·10 ⁻³
	5	6.23	105.8	1.00·10 ⁷	106.7	165.90	5.05	0.997	4.99·10 ⁷	3.37	0.943	1.80·10 ⁻³
	6	6.14	112.3	1.08·10 ⁷	112.8	188.18	4.95	1.000	3.52·10 ⁸	3.24	0.943	1.15·10 ⁻³
	7	6.16	118.7	1.06·10 ⁷	119.3	198.21	5.02	1.000	3.07·10 ⁸	3.27	0.943	1.13·10 ⁻³
BSA	1	7.40	93.3	4.76·10 ⁶	93.5	3.83·10 ⁶	25.42	0.933	2.44·10 ⁶	14.16	1.000	1.19·10 ⁻³
	2	6.90	88.6	4.76·10 ⁶	88.9	3.46·10 ⁶	28.07	0.923	2.65·10 ⁶	12.30	1.000	4.45·10 ⁻⁴
	3	6.84	87.4	4.65·10 ⁶	87.6	3.26·10 ⁶	31.05	0.916	2.77·10 ⁶	11.67	1.000	4.26·10 ⁻⁴
	4	6.78	88.0	4.59·10 ⁶	88.2	3.10·10 ⁶	32.96	0.912	2.88·10 ⁶	11.30	1.000	3.94·10 ⁻⁴
	5	6.78	87.6	4.56·10 ⁶	87.8	3.07·10 ⁶	32.92	0.912	2.85·10 ⁶	11.31	1.000	3.92·10 ⁻⁴
	6	6.78	85.7	4.09·10 ⁶	85.9	3.01·10 ⁶	26.85	0.925	2.52·10 ⁶	12.27	1.000	2.03·10 ⁻⁴
	7	6.76	84.5	4.10·10 ⁶	84.7	3.00·10 ⁶	26.68	0.927	2.46·10 ⁶	12.47	1.000	2.00·10 ⁻⁴
FBS	1	7.97	95.9	2.45·10 ⁶	97.1	1.27·10 ⁶	12.25	0.983	2.44·10 ⁶	55.36	0.928	1.28·10 ⁻³
	2	7.71	95.5	2.77·10 ⁶	96.6	9.24·10 ⁵	13.61	0.973	2.44·10 ⁶	34.59	0.961	2.33·10 ⁻³
	3	7.74	94.7	2.68·10 ⁶	95.8	9.72·10 ⁵	13.26	0.971	2.32·10 ⁶	38.73	0.961	2.32·10 ⁻³
	4	7.64	95.2	2.85·10 ⁶	96.3	8.04·10 ⁵	14.46	0.974	2.67·10 ⁶	29.91	0.957	2.73·10 ⁻³
	5	7.51	94.1	3.30·10 ⁶	95.1	5.97·10 ⁵	16.91	0.980	3.42·10 ⁶	22.00	0.955	2.91·10 ⁻³
	6	7.58	93.0	3.12·10 ⁶	94.0	5.32·10 ⁵	17.64	0.983	3.19·10 ⁶	21.40	0.953	2.60·10 ⁻³
	7	7.60	91.6	3.01·10 ⁶	92.7	4.76·10 ⁵	18.33	0.986	3.06·10 ⁶	20.51	0.952	2.25·10 ⁻³

In the presence of glucose the physical arrangement of the electrical equivalent circuit has slightly changed to get the best fitting. The physical arrangement of the electrical equivalent circuit in the presence of glucose to get the best fitting has slightly changed. Taking into account the high resolution XPS spectra, some P and Ca elements could be seen on the TT-Ti surface (Table 2), indicating that the covering by glucose is not complete. That's means that some of the surface is free to be in contact with the other components of the electrolyte. In order to fit the experimental data, a new electronic

components associated with a second time constant to simulate the presence of glucose in the interface electrolyte/TT-Ti surfaces has been included. In this case, circuit in Figure 6b is considered. The CPE2 values are constant over testing time, indicating that glucose adsorption on the titanium surface is very fast (Fig. 7). From the first day practically all the surface is covered by glucose. The CPE1 values remains practically constant with a slight trend to decrease its value. This trend is followed by R1 with a slight decrease over testing time, indicating that the glucose adsorbed on the titanium does not prevent

the ionic diffusion to improve the resistance of oxidized surface. On the other hand, the addition of glucose to the solution is more sensitive to the CPE1 value that takes lower values than in the case of P and PCa solutions.

The change in R1 over immersion time of TT-Ti in P, PCa and PCaG solutions agrees with the results obtained by Contu *et al.* (2002). These authors assume that the passive film on Ti and Ti-alloys grows following an ionic mechanism whereby oxygen ions (O^{2-}) diffuse from the passive film-electrolyte interface toward the metal-passive film interface.

When titanium is immersed in a solution containing BSA the circuit of Figure 6c is considered (Fig. 7). Again, taking into account the high resolution XPS spectra, neither P nor Ca could be seen on the TT-Ti surface (Table 2), indicating that the covering by BSA seems to be complete and both time constants can be separated in the equivalent circuit. In this case, it is remarkable to note that the value of CPE2 increases with respect to glucose solution in one order of magnitude, indicating that the protein layer on the oxidized surface is less compact or more conductive than the glucose layer adhered on the oxidized surface, allowing to spread ions through it (Uchida *et al.*, 2003). Surprisingly, R2 values are several orders of magnitude higher than in the case of glucose. However, comparing R2 and R1 in BSA solution, the very similar values are indicating that both time constants are very close and there is an overlapping between them and it is very difficult to isolate both contributions. BSA seems to create a more dynamic and active layer on the oxidized surface because the comparison of R1 with respect to those values obtained with P, PCa and BSA solutions gives a difference of more than one order of magnitude. BSA is able to reduce significantly the resistance of the oxide layer maybe due to the organometallic complex formation. Nevertheless, in literature has been published that these ions could remove BSA molecules, adsorb on the surface and form CaP deposits but at longer times (Mantel and Wightman, 1994).

Finally, when TT-Ti samples are immersed in the FBS the impedance plots are very similar to those obtained for the BSA and the impedance spectra are adequately fitted by using the same equivalent circuit. The contribution of P and Ca incorporated into the passive film is so low (comparing P and Ca intensities for solutions containing glucose and FBS) that the best equivalent circuit to fit the experimental data is described in Figure 6c. In Figure 7 can be seen that the values of CPE2 slightly increases and R2 decrease over immersion time. On the other hand, R1 value slowly increases and CPE1 decreases considerably with immersion time. Comparing the R2 and CPE2 with those obtained in BSA solution, it can be seen that are lower than

in BSA solution. R1 is around the same value than in BSA solution and CPE1 takes the highest values of all the media tested. The corrosion behaviour of oxidized Ti immersed in FBS is practically the same as in BSA solutions. The low R1 values indicate that proteins, in this case albumin, are able to active the oxidized surface of Ti. The decrease of R1 in both cases (Fig. 7) could be related according to Williams *et al.* (1988) with the ability of proteins to form complex with titanium ions. However, the multitude of other compounds that are included in the FBS medium has an influence on the electrochemical properties of the interface created between oxidized surface and solution. This effect is especially seen in the capacitance values of the oxide surface/medium interface.

4.3. Polarization curves

Figure 8 shows the polarization curves with respect to the corrosion potential of TT-Ti (polarization-i) after seven days of immersion in each solution.

With respect to the anodic polarization from E_{corr} , the passive region does not show significant

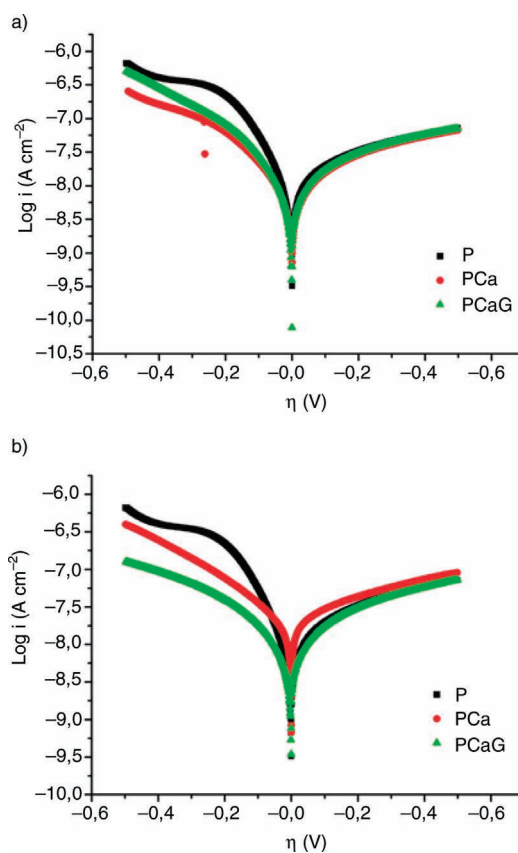


FIGURE 8. Linear polarization curves of a) P/TT-Ti (■), PCa/TT-Ti (●) and PCaG/Ti-TT (▲); and b) BSA/TT-Ti (●), FBS/Ti-TT (▲), after 7 days of immersion.

differences between the polarization curves (Fig. 8a and b). All of them draw passive regions with stable current densities that slightly increase as polarization does. However, among of them, BSA seems to show the most active behaviour, especially at the surrounding of corrosion potential, at the beginning of anodic polarization.

On the other hand, two regions can be identified in the cathodic part of the polarization curve when TT-Ti is immersed in the P, PCa and PCaG solutions (Fig. 8a). The first one, between -0.500 V and -0.200 V, can be attributed to the combination of oxygen and hydrogen reduction, based on the pH/potential diagram for Ti at $\text{pH}=7,4$; and the second one, between -0.200 V and the corrosion potential, is attributed to the reduction of oxygen dissolved in the solution. The addition of Ca to the P solution results in a significant decrease in current in the cathodic range with an increase in the Tafel slope (Table 4). In the presence of glucose, the cathodic polarization curve obtained for oxygen reduction is practically the same as that of PCa solution (Fig. 8a). The cathodic Tafel slope obtained for P solution was 0.121 V corresponding to a mechanism with two steps. The first one is the formation of H_2O_2 and the second one water formation, both of them with a charge transfer of two electrons. The cathodic Tafel slopes obtained for PCa and PCaG solutions were -0.187 and -0.160 V respectively, so both solutions prevent the formation of H_2O_2 and H_2O .

The Figure 8b shows the polarization curves in presence of P, BSA and FBS solutions. The cathodic current of TT-Ti immersed in FBS is decreased with respect to the TT-Ti immersed in P, PCa, PCaG solution and BSA. This indicates that the reduction of oxygen and hydrogen is more impeded on the surface of TT-Ti in FBS. With respect to the Tafel slopes, in BSA and FBS cases, cathodic slopes are higher than in the presence of P, PCa and PCaG solutions. This indicates that the cathodic control is more accused in the presence of organic compounds due probably to the adsorption of proteins, such as albumin, on the surface.

In summary, the electrochemical properties of the physiological medium/TT-Ti surface are

TABLE 4. Tafel slopes and open circuit potentials from polarization curves of P/TT-Ti, PCa/Ti-TT, PCaG/Ti-TT, BSA/Ti-TT and FBS/Ti-TT samples

Solutions	E_{corr} (V)	b_a (V)	b_c (V)
P	0.038	0.466	0.121
PCa	0.079	0.421	0.187
PCaG	0.104	0.360	0.160
BSA	-0.082	0.454	0.228
FBS	-0.081	0.416	0.213

completely controlled by the formation of a homogeneously distributed enriched TiO_2 surface that provides a high corrosion resistance, even in the presence of proteins that seems to be able to react with the Ti lead to the organometallic complex and producing some decrease in the oxide resistance.

5. CONCLUSIONS

Each component of the culture medium interacts with the TT-Ti surface in different ways:

The Ca and P of the physiological medium are incorporated to the titanium oxide layer slightly increasing the corrosion resistance.

The BSA covers the Ti surface independently of the presence of calcium ions in the solution. The adsorption of BSA in the presence of calcium and phosphate ions inhibits the oxygen diffusion to the electrode surface.

The TT-Ti surface interacts with albumin and fetal bovine serum probably giving rise to the formation of organometallic complex.

ACKNOWLEDGMENTS

The authors thank the financial support under project MAT2011-29152-C02-01.

REFERENCES

- Albrektsson, T., Johansson, C., Sennerby, L. (1994). Biological aspects of implant dentistry: osseointegration. *Periodontology* 2000 4 (1), 58–73. <http://dx.doi.org/10.1111/j.1600-0757.1994.tb00006.x>.
- Alonso, C., García-Alonso, M.C., Escudero, M.L. (2008). Patent N° 200801041, *Célula electrolítica para estudio de la interfase formada por un implante metálico en medio celular y procedimiento de utilización de dicha célula electrolítica*, España.
- Bello-Samir, A., de Jesús-Maldonado, I., Rosim-Fachini, E., Sundaram-Paul A., Diffoot-Carlo, N. (2010). In vitro evaluation of human osteoblast adhesion to a thermally oxidized γ -TiAl intermetallic alloy of composition Ti-48Al-2Cr-2Nb (at.%). *J. Mater. Sci.: Mater. Med.* 21 (5), 1739–1750. <http://dx.doi.org/10.1007/s10856-010-4016-6>.
- Browne, M., Gregson, P.J. (1994). Surface modification of Titanium alloy implants. *Biomaterials* 15 (11), 894–898. [http://dx.doi.org/10.1016/0142-9612\(94\)90113-9](http://dx.doi.org/10.1016/0142-9612(94)90113-9).
- Burgos-Asperilla, L., García-Alonso, M.C., Escudero, M.L., Alonso, C. (2010). Study of the interaction of inorganic and organic compounds of the body fluids with Ti surface. *Acta Biomater.* 6 (2), 652–661. <http://dx.doi.org/10.1016/j.actbio.2009.06.019>.
- Carboneras, M., Iglesias, C., Pérez-Maceda, B.T., del Valle, J.A., García-Alonso, M.C., Alobera, M.A., Clemente, C., Rubio, J.C., Escudero, M.L., Lozano, R.M. (2011). Comportamiento frente a la corrosión y biocompatibilidad in vitro/in vivo de la aleación AZ31 modificada superficialmente. *Rev. Metal.* 47 (3), 212–223. <http://dx.doi.org/10.3989/revmetalm.1065>.
- Clark, P., Connolly, P., Curtis, A.S.G., Dow, J.A.T., Wilkinson, C.D.W. (1991). Cell guidance by ultrafine topography in vitro. *J. Cell. Sci.* 99, 73–77.
- Contu, F., Elsener, B., Böhni, H. (2002). Characterization of implant materials in fetal bovine serum and sodium sulfate by electrochemical impedance spectroscopy. I.

- Mechanically polished samples. *J. Biomed. Mater. Res.* 62 (3), 412–421. <http://dx.doi.org/10.1002/jbm.10329>.
- Curtis, A.S.G., Varde, M. (1964). Control of Cell Behavior: Topological Factors. *J. Natl. Cancer Inst.* 33 (1), 15–26. <http://dx.doi.org/10.1093/jnci/33.1.15>.
- Dalby, M.J., Riehle, M.O., Johnstone, H., Affrossman, S., Curtis, A.S.G. (2004). Investigating the limits of filopodial sensing: a brief report using SEM to image the interaction between 10 nm high nano-topography and fibroblast filopodia. *Cell. Biol. Int.* 28 (3), 229–236. <http://dx.doi.org/10.1016/j.cellbi.2003.12.004>.
- Den Braber, E.T., de Ruijter, J.E., Ginsel, L.A., von Recum, A.F., Jansen, J.A. (1996). Quantitative analysis of fibroblast morphology on microgrooved surfaces with various groove and ridge dimension. *Biomaterials* 17 (21), 2037–2044. [http://dx.doi.org/10.1016/0142-9612\(96\)00032-4](http://dx.doi.org/10.1016/0142-9612(96)00032-4).
- Ducheyne, P., Healy, K.E. (1991). *Titanium: Immersion-induced surface chemistry changes and the relationship to passive dissolution and bioactivity in The Bone–Biomaterial Interface*, Davies, J.E. (Ed), University of Toronto Press, pp. 62–67.
- Ellingsen, J.E. (1991). A study on the mechanism of protein adsorption to TiO₂. *Biomaterials* 12 (6), 593–596. [http://dx.doi.org/10.1016/0142-9612\(91\)90057-H](http://dx.doi.org/10.1016/0142-9612(91)90057-H).
- Escudero, M.L., Muñoz-Morris, M.A., García-Alonso, M.C., Fernández-Escalante, E. (2004). In vitro evaluation of γ -TiAl intermetallic for potential endoprosthesis applications. *Intermetallics* 12 (3), 253–260. <http://dx.doi.org/10.1016/j.intermet.2003.10.004>.
- García-Alonso, M.C., Saldana, L., Valles, G., González-Carrasco, J.L., González-Cabrero, J., Martínez, M.E., Gil-Garay, E., Munuera, L. (2003). In vitro corrosion behaviour and osteoblast response to thermally oxidized Ti6Al4V alloy. *Biomaterials* 24 (1), 19–26. [http://dx.doi.org/10.1016/S0142-9612\(02\)00237-5](http://dx.doi.org/10.1016/S0142-9612(02)00237-5).
- Hanawa, T., Ota, M. (1991). Calcium-phosphate naturally formed on titanium in electrolyte solution. *Biomaterials* 12 (8), 767–774. [http://dx.doi.org/10.1016/0142-9612\(91\)90028-9](http://dx.doi.org/10.1016/0142-9612(91)90028-9).
- Healy, K.E., Ducheyne, P. (1992). Hydration and preferential molecular adsorption on titanium in vitro. *Biomaterials* 13 (8), 553–561. [http://dx.doi.org/10.1016/0142-9612\(92\)90108-Z](http://dx.doi.org/10.1016/0142-9612(92)90108-Z).
- Horcas, I., Fernández, R., Gómez-Rodríguez, J.M., Colchero, J., Gómez-Herrero, J., Baro, A.M. (2007). WSXM: A software for scanning probe microscopy and a tool for nanotechnology. *Rev. Sci. Instrum.* 78, 013705. <http://dx.doi.org/10.1063/1.2432410>.
- Hughes-Wassell, D.T., Embery, G. (1996). Adsorption of bovine serum albumin on to titanium powder. *Biomaterials* 17 (9), 859–864. [http://dx.doi.org/10.1016/0142-9612\(96\)83280-7](http://dx.doi.org/10.1016/0142-9612(96)83280-7).
- Hwang, K.S., Lee, Y.H., Kang, B.A., Kim, S.B., Oh, J.S. (2003). Effect of annealing titanium on in vitro bioactivity. *J. Mater. Sci. - Mater. M.* 14 (6), 521–529. <http://dx.doi.org/10.1023/A:1023408030405>.
- Jones D.B. (1998). Cells and Metals in *Metals as biomaterials*, Helsen, J.A., Breme H.J. (Ed.) Wiley, J., & Sons, Chichester, England, pp. 317–335.
- Kasemo, B. (2002). Biological surface science. *Surf. Sci.* 500, 656–677. [http://dx.doi.org/10.1016/S0039-6028\(01\)01809-X](http://dx.doi.org/10.1016/S0039-6028(01)01809-X).
- Kubo, K., Tsukimura, N., Iwasa, F., Ueno, T., Saruwatari, L., Aita, H., Chiou, W.A., Ogawa, T. (2009). Cellular behavior on TiO₂ nanonodular structures in a micro-to-nanoscale hierarchy model. *Biomaterials* 30 (29), 5319–5329. <http://dx.doi.org/10.1016/j.biomaterials.2009.06.021>.
- Lima, J., Sousa, S.R., Ferreira, A., Barbosa, M.A. (2001). Interactions between calcium, phosphate, and albumin on the surface of titanium. *J. Biomed. Mater. Res.* 55 (1), 45–53. [http://dx.doi.org/10.1002/1097-4636\(200104\)55:13.3.CO;2-S](http://dx.doi.org/10.1002/1097-4636(200104)55:13.3.CO;2-S).
- Lin, D., Li, Q., Li, W., Ichim, I., Swain, M. (2007). Damage Evaluation of Bone Tissues with Dental Implants. *Advances in Fracture and Damage Mechanics VI*, 905–908. <http://dx.doi.org/10.4028/www.scientific.net/KEM.348-349.905>.
- Lord, M.S., Foss, M., Besenbacher, F. (2010). Influence of nanoscale surface topography on protein adsorption and cellular response. *Nano Today* 5 (1), 66–78. <http://dx.doi.org/10.1016/j.nantod.2010.01.001>.
- Lu, G., Bernasek, S.L., Schwartz, J. (2000). Oxidation of a polycrystalline titanium surface by oxygen and water. *Surf. Sci.* 458 (1–3), 80–90. [http://dx.doi.org/10.1016/S0039-6028\(00\)00420-9](http://dx.doi.org/10.1016/S0039-6028(00)00420-9).
- Mantel, M., Wightman, J.P. (1994). Influence of the surface-chemistry on the wettability of stainless-steel. *Surf. Interface Anal.* 21 (9), 595–605. <http://dx.doi.org/10.1002/sia.740210902>.
- Mareci, D., Lucero, V., Mirza, J. (2009). Effect of replacement of vanadium by iron on the electrochemical behaviour of titanium alloys in simulated physiological media. *Rev. Metal.* 45, 32–41. <http://dx.doi.org/0.3989/revmetalm.0750>.
- McCafferty, E., Wightman, J.P. (1999). An X-Ray photoelectron spectroscopy sputter profile study of the native air-formed film on titanium. *Appl. Surf. Sci.* 143 (1–4), 92–100. [http://dx.doi.org/10.1016/S0169-4332\(98\)00927-1](http://dx.doi.org/10.1016/S0169-4332(98)00927-1).
- Muñoz, A.I., Mischler, S. (2007). Interactive Effects of Albumin and Phosphate Ions on the Corrosion of CoCrMo Implant Alloy. *J. Electrochem. Soc.* 154 (10), C562–570. <http://dx.doi.org/10.1149/1.2764238>.
- Ouerd, A., Alemany-Dumont, C., Belthome, G., Normand, B., Szunerits, S. (2007). Reactivity of titanium in physiological medium: electrochemical characterization of the metal/protein interface. *J. Electrochem. Soc.* 154 (10), C593–C601. <http://dx.doi.org/10.1149/1.2769819>.
- Ratner, B.D. (2004). *Biomaterials Science: an Introduction to Materials in Medicine*. 2nd Edition. Elsevier Academic Press (Ed.), Amsterdam, Boston.
- Rechendorff, K., Hovgaard, M.B., Foss, M., Zhdanov, V.P., Besenbacher, F. (2006). Enhancement of protein adsorption induced by surface roughness. *Langmuir* 22 (22), 10885–10888. <http://dx.doi.org/10.1021/la0621923>.
- Rubio, J.C., García-Alonso, M.C., Alonso, C., Alobera, M.A., Clemente, C., Munuera, L., Escudero, M.L. (2008). Determination of metallic traces in kidneys, livers, lungs and spleens of rats with metallic implants after a long implantation time. *J. Mater. Sci. Mater. Med.* 19 (1), 369–375. <http://dx.doi.org/10.1007/s10856-007-3002-0>.
- Saldana, L., Vilaboa, N., Valles, G., González-Cabrero, J., Munuera, L. (2005). Osteoblast response to thermally oxidized Ti6Al4V alloy. *J. Biomed. Mater. Res.* 73A(1), 97–107. <http://dx.doi.org/10.1002/jbm.a.30264>.
- Serro, A.P., Fernandes, A.C., Saramago, B., Lima, J., Barbosa, M.A. (1997). Apatite deposition on titanium surfaces—the role of albumin adsorption. *Biomaterials* 18 (4), 963–968. [http://dx.doi.org/10.1016/S0142-9612\(97\)00031-8](http://dx.doi.org/10.1016/S0142-9612(97)00031-8).
- Serro do, A.P.V.A., Fernandes A.C., de Jesus B., Saramago V. (1997). The influence of proteins on calcium phosphate deposition over titanium implants studied by dynamic contact angle analysis and XPS. *Colloid. Surface B* 10 (2), 95–104. [http://dx.doi.org/10.1016/S0927-7765\(97\)00060-X](http://dx.doi.org/10.1016/S0927-7765(97)00060-X).
- Sundgren, J.E., Bodo, P., Lundstrom, I. (1986). Auger electron spectroscopic studies of the interface between human tissue and implants of titanium and stainless steel. *J. Colloid Interf. Sci.* 110 (1), 9–20. [http://dx.doi.org/10.1016/0021-9797\(86\)90348-6](http://dx.doi.org/10.1016/0021-9797(86)90348-6).
- Uchida, M., Kim, H.M., Kokubo, T., Fujibayashi, S., Nakamura, T. (2003). Structural dependence of apatite formation on titania gels in a simulated body fluids. *J. Biomed. Mater. Res.* 64A, 164–170. <http://dx.doi.org/10.1002/jbm.a.10414>.
- Vaquila, I., Passetgi Jr, M.C.G., Ferron, J. (1996). Temperature effect in the early stages of titanium oxidation. *Appl. Surf. Sci.* 93 (3), 247–253. [http://dx.doi.org/10.1016/0169-4332\(95\)00334-7](http://dx.doi.org/10.1016/0169-4332(95)00334-7).
- Wagner, C.D., Davis, L.E., Zeller, M.V., Taylor, J.A., Raymond, R.H., Gale, L.H. (1981). Empirical atomic sensitivity

- factors for quantitative analysis by electron spectroscopy for chemical analysis. *Surf. Interface Anal.* 3 (5), 211–225. <http://dx.doi.org/10.1002/sia.740030506>.
- Wagner, C. D., Riggs, W.M., Davis, L.E., Moulder, J.F., Mulinberg, G.E. (1992). *Handbook of X-ray photoelectron spectroscopy*, Perkin-Elmer Corporation, Physical Electronics Division (Eds.), Eden Prairie, Minnesota, USA.
- Williams, R.L., Brown, S.A., Merritt, K. (1988). Electrochemical studies on the influence of proteins on the corrosion of implant alloys. *Biomaterials* 9 (2), 181–186. [http://dx.doi.org/10.1016/0142-9612\(88\)90119-6](http://dx.doi.org/10.1016/0142-9612(88)90119-6).
- Wojciak-Stothard, B., Madeja, Z., Korohoda, W., Curtis, A., Wilkinson, C. (1995). Activation of macrophage-like cells by multiple grooved substrata. Topographical control of cell behavior. *Cell Biol. Int.* 19 (6), 485–490. <http://dx.doi.org/10.1006/cbir.1995.1092>.